^{18}F-FDG PET Database of Longitudinally Confirmed Healthy Elderly Individuals Improves Detection of Mild Cognitive Impairment and Alzheimer's Disease

Lisa Mosconi[1], Wai Hon Tsui[1,2], Alberto Pupi[3], Susan De Santi[1], Alexander Drzezga[4], Satoshi Minoshima[5], and Mony J. de Leon[1,2]

[1]New York University School of Medicine, New York, New York; [2]Nathan Kline Institute, New York, New York; [3]University of Florence, Florence, Italy; [4]University of Munich, Munich, Germany; and [5]University of Washington, Seattle, Washington

The normative reference sample is crucial for the diagnosis of Alzheimer's disease (AD) with automated ^{18}F-FDG PET analysis. We tested whether an ^{18}F-FDG PET database of longitudinally confirmed healthy elderly individuals (''normals,'' or NLs) would improve diagnosis of AD and mild cognitive impairment (MCI). **Methods:** Two ^{18}F-FDG PET databases of 55 NLs with 4-y clinical follow-up examinations were created: one of NLs who remained NL, and the other including a fraction of NLs who declined to MCI at follow-up. Each ^{18}F-FDG PET scan of 19 NLs, 37 MCI patients, and 33 AD patients was *z* scored using automated voxel-based comparison to both databases and examined for AD-related abnormalities. **Results:** Our database of longitudinally confirmed NLs yielded 1.4- to 2-fold higher *z* scores than did the mixed database in detecting ^{18}F-FDG PET abnormalities in both the MCI and the AD groups. ^{18}F-FDG PET diagnosis using the longitudinal NL database identified 100% NLs, 100% MCI patients, and 100% AD patients, which was significantly more accurate for MCI patients than with the mixed database (100% NLs, 68% MCI patients, and 94% AD patients identified). **Conclusion:** Our longitudinally confirmed NL database constitutes reliable ^{18}F-FDG PET normative values for MCI and AD.

Key Words: neurology; PET; Alzheimer's disease; normative reference database; early diagnosis

J Nucl Med 2007; 48:1129–1134
DOI: 10.2967/jnumed.107.040675

Measurement of the cerebral metabolic rate of glucose (CMRglc) with ^{18}F-FDG PET is being increasingly used to support the clinical diagnosis of Alzheimer's disease (AD). Compared with age-matched healthy elderly individuals ("normals," or NLs), AD patients present with characteristic regional CMRglc reductions in the posterior cingulate and parietotemporal cortices (*1*). Patients with mild cognitive impairment (MCI) at high risk for developing AD (*2*) also show a similar pattern of hypometabolism, although the magnitude and extent of CMRglc reductions are milder than in AD (*3,4*).

Precise detection of hypometabolism in AD and MCI patients may contribute to the clinical diagnosis, particularly in the early stages of AD, when clinical symptoms are not fully expressed. Automated methods of diagnostic image analysis have been developed to facilitate ^{18}F-FDG PET evaluations of single patient's scans with respect to a normative database by producing an observer-independent quantitative mapping of regional CMRglc abnormalities (*5–7*). Whether regional CMRglc is considered abnormal is therefore directly related to the choice of the appropriate normative reference sample.

Evidence shows that progressive CMRglc reductions and atrophy in AD-affected brain regions are present in elderly individuals years before a decline to MCI or AD occurs (*8–12*). On ^{18}F-FDG PET, such CMRglc reductions significantly involve the association cortices that are typically inspected to diagnose AD (*8,9,12*). These results raise concerns about the definition of "normality" and suggest that a database comprising baseline NLs of unknown clinical outcome might include ^{18}F-FDG PET scans with preclinical CMRglc alterations. Such a baseline database would increase variance and decrease the sensitivity for detecting CMRglc abnormalities in clinical patients at mild stages of disease. To our knowledge, none of the currently available ^{18}F-FDG PET databases were created to include subjects who were known to have remained healthy over time.

The present study showed that using a reference ^{18}F-FDG PET database of longitudinally confirmed NLs improves the accuracy in diagnosing mild AD and MCI.

Received Feb. 13, 2007; revision accepted Apr. 5, 2007.
For correspondence contact: Lisa Mosconi, PhD, Center for Brain Health of the Silberstein Institute, Department of Psychiatry, NYU School of Medicine, 560 First Ave., New York NY, 10016.
E-mail: lisa.mosconi@med.nyu.edu

MATERIALS AND METHODS

Subjects

This study included 96 NLs, 37 MCI patients, and 33 AD patients examined at New York University and at the University of Florence. Both centers administer several identical neuropsychological tests; use comparable criteria for the definition of normality, MCI, and AD; follow the recommendations of the National Institute of Neurological and Communicable Disease and Stroke–Alzheimer's Disease and Related Disorders Association (NINCDS-ADRDA) workgroup and the Diagnostic and Statistical Manual of Mental Disorders (DSM)–IV criteria for the diagnosis of AD; and use common standardized imaging acquisition protocols, as previously described (*13*).

All participants or caregivers provided written informed consent, and the subjects were studied with the approval of the Institutional Review Board. The subjects underwent clinical, medical, neuropsychological, and CT or MRI examinations and routine blood analysis; were 50–83 y old; had no evidence of stroke, clinically uncontrolled diabetes, major head trauma, or depression; and used no cognitively active medications. NLs had no evidence of functional impairment based on extensive clinical interviews, a Clinical Dementia Rating of 0 (*14*) or Global Deterioration Scale of 1 or 2 (*15*), and a Mini-Mental State Examination (MMSE) score of at least 28. AD patients fulfilled NINCDS-ADRDA and DSM-IV criteria for probable AD, had significant deficits in activities of daily living, deficits in 2 or more cognitive domains, and a Clinical Dementia Rating of at least 1. AD was classified as mild (Clinical Dementia Rating of 1, $n = 15$) or as moderate to severe (Clinical Dementia Rating of at least 2, $n = 18$). Amnesic MCI patients had normal activities of daily living and general intelligence, no dementia, a Clinical Dementia Rating of 0.5 or Global Deterioration Scale of 3, an MMSE score of at least 24, and memory scores 1.5 SDs below norms (*2*). The neuropsychological testing battery included the MMSE, immediate and delayed recall of a paragraph and paired associates, the designs test, the object-naming test, and the Wechsler Adult Intelligence Scale–Revised (*12,13*). For all these tests, normative reference values exist (*16*).

Database Development

Seventy-seven NLs received clinical follow-up examinations and were examined for a change in clinical status after 4 ± 1 y. At the follow-up, 2 groups were identified: 55 NLs that remained NL (NL-NLs), and 22 NLs that declined to MCI (NL-MCI patients). These subjects were reported on previously (*8,12*) and were now used to develop two ^{18}F-FDG PET normative databases of 55 subjects each: DB$^+$ (a database of baseline scans of only NL-NLs) and DB$^-$ (a database of baseline scans of an epidemiologically likely fraction of NL-MCI patients, in keeping with an estimated rate of decline from NL to MCI or AD of ~10%/y (*8–12*)). With an aggregate 4-y risk of 10%, DB$^-$ comprised 22 (40% of 55) NL-MCI patients and 33 randomly selected NL-NLs. DB$^+$ comprised the 55 NL-NLs. Subjects in both databases had demographic characteristics appropriate for studies on AD (Table 1). The ^{18}F-FDG PET scans of the remaining 19 NLs, 37 MCI patients, and 33 AD patients were used to examine the accuracy of the 2 databases in detecting disease.

^{18}F-FDG PET Acquisition

All subjects underwent ^{18}F-FDG PET using standardized procedures within 3 mo of the clinical examinations. The studies were performed in a dimly lit room with minimal background noise after an intravenous injection of 140–370 MBq of ^{18}F-FDG. Scanning began 40 min after injection and continued for 20 min. Images were reconstructed using filtered backprojection, including correction for attenuation and scatter, using standard software as supplied by scanner manufacturers. PET scans at New York University were acquired on a ECAT 931 scanner (Siemens; 6.2-mm in-plane full width at half maximum; 6.75-mm interslice distance). Two 15-slice acquisitions translated by a half-slice thickness (~3.4 mm) were interleaved for a final slice thickness of 4.25 mm. PET scans at the University of Florence were acquired on an Advance scanner (GE Healthcare; 4.6-mm in-plane full width at half maximum; 4.25-mm slice thickness).

^{18}F-FDG PET Image Analysis

^{18}F-FDG PET scans were processed using Neurologic Statistical Image Analysis software (Neurostat; Washington University) (*3,5*). Each image was warped to the common stereotactic coordinate system, and the 2 databases were created using the spatially normalized ^{18}F-FDG PET scans of 55 longitudinally confirmed NL-NLs (DB$^+$) and 22 NL-MCI patients and 33 NL-NLs (DB$^-$). Each spatially normalized scan of the remaining NLs, MCI patients, and AD patients was compared with both DB$^+$ and DB$^-$ after adjusting for global CMRglc at $P \leq 0.05$ (1-sided), corresponding to $z \geq 1.64$. z scores ($z = x_{subject} - mean_{database})/SD_{database}$) are reported in absolute values. Gray-matter activities

TABLE 1
Clinical Characteristics of Participants

Characteristic	Reference database		Clinical groups			
	DB$^-$	DB$^+$	NL	MCI	Mild AD	Moderate-to-severe AD
n	55	55	19	37	15	18
Age* (y)	69 (7), 50–82	68 (7), 50–80	68 (4), 55–80	70 (7), 50–82	69 (8), 50–83	65 (7), 51–80
Education* (y)	15 (2), 12–18	15 (2), 12–18	14 (3), 11–18	11 (4), 8–18†	12 (3), 9–18†	10 (3), 8–18†
% Female	55	56	58	60	53	67
MMSE*	29 (1), 28–30	29 (1), 28–30	29 (1), 28–30	27 (2), 24–30	26 (2), 24–28	19 (4), 10–23†‡§

*Values are mean, with SD in parentheses, followed by range.
†Lower than NL, $P \leq 0.05$.
‡Lower than MCI, $P \leq 0.05$.
§Lower than mild AD, $P \leq 0.05$.

were extracted to predefined surface pixels using a 3-dimensional stereotactic surface projection technique (3D-SSP), which minimized residual anatomic variances across subjects and partial-volume effects, yielding robust voxel-based statistical analysis (*3,5*).

Bilateral standardized regions of interest (ROIs) (inferior parietal lobe, lateral temporal lobe, posterior cingulate cortex, prefrontal cortex, occipital cortex, and sensorimotor cortex; Fig. 1) were applied to 3D-SSP maps to extract mean ROI z scores and generate regional numeric indices representing the degree of CMRglc abnormalities (*4*). All 3D-SSP maps were inspected by 2 raters and classified as positive or negative for CMRglc abnormalities consistent with AD based on detection of hypometabolism in the posterior cingulate, parietotemporal, or frontal cortex, with sparing of the sensorimotor cortex, occipital cortex, and cerebellum (*1,3,4*), using published protocols with known intra- and interrater reliabilities (*1,13,17*). The final diagnosis was made by joint agreement. Classification was facilitated by detection of hypometabolic patterns exceeding the predefined z score threshold within each ROI superimposed on the 3D-SSP maps (Fig. 1) (*4*).

Statistical Analysis

The general linear model with post hoc t tests and χ^2 tests was used to examine clinical and ROI z score measures between groups and databases. The effects of the 2 databases in distinguishing AD and MCI groups from NLs were compared. Receiver operator characteristic curves and logistic regressions were used to examine z scores and the resulting ^{18}F-FDG PET diagnosis from the 2 databases in distinguishing AD and MCI patients from NLs. The results were examined at $P < 0.05$. Analyses were done using SPSS, version 12.0 (SPSS Inc.).

RESULTS

The groups did not differ in age or sex (Table 1). Education was lower in the MCI and AD patients than in any NL groups ($P < 0.05$). MMSE scores were lower in AD patients than in NLs and MCI patients. MMSE scores were lower in patients with moderate-to-severe AD than in patients with mild AD ($P \leq 0.01$).

Significant differences between the 2 databases were found in detecting hypometabolism in MCI and AD patients (Table 2). z scores were generally higher (reflecting greater CMRglc reductions) for DB$^+$ than for DB$^-$, reaching statistical significance in both inferior parietal lobes, the posterior cingulate cortex, and the right lateral temporal lobe in MCI patients and in both inferior parietal lobes, the lateral temporal lobe, and the posterior cingulate cortex in AD patients ($P \leq 0.05$; Table 2). z scores were significantly higher for DB$^+$ than DB$^-$ for both the mild and the moderate-to-severe AD groups (Table 2). The effect in distinguishing disease from lack of disease was larger for DB$^+$ than for DB$^-$ in all ROIs (Fig. 2).

Within these ROIs, DB$^+$ z scores yielded significantly higher group discrimination accuracies than did DB$^-$ z scores ($P < 0.05$). For NL versus MCI, DB$^+$ z scores yielded accuracies of 91% (right) and 99% (left) for the inferior parietal lobe and 99% (right) and 100% (left) for the posterior cingulate cortex, whereas DB$^-$ z scores had accuracies of 78% (right) and 89% (left) for the inferior parietal lobe and 78% (right) and 92% (left) for the posterior cingulate cortex. Although DB$^+$ z scores for the right lateral temporal lobe were higher than DB$^-$ z scores, the diagnostic accuracy of the lateral temporal lobe z scores was comparable between databases, at 95%. For NLs versus patients with mild AD, DB$^+$ z scores yielded accuracies of 92% (right) and 99% (left) for the inferior parietal lobe, 98% (right) and 100% (left) for the posterior cingulate cortex, and 95% for both the left and the right lateral temporal lobes, whereas DB$^-$ z scores had accuracies of 82% (right) and 87% (left) for the inferior parietal lobe, 78% (right) and 92% (left) for the posterior cingulate cortex, and 90% (right) and 95% (left) for the lateral temporal lobe ($P < 0.05$). For NLs versus patients with moderate to severe AD, DB$^+$ z scores were more accurate than DB$^-$ z scores in only the right hemisphere for the inferior parietal lobe (DB$^+$, 91%; DB$^-$, 84%), the posterior cingulate cortex (DB$^+$, 100%; DB$^-$, 87%), and the lateral temporal lobe (DB$^+$, 98%; DB$^-$, 92%) ($P < 0.05$).

^{18}F-FDG PET diagnosis identified all 19 NLs (100%) as negative for disease with both databases. Using DB$^-$, a positive PET diagnosis was made in 31 (94%) of 33 AD patients and 25 (68%) of 37 MCI patients (Fig. 3). A negative PET diagnosis was more frequent in MCI patients than in AD patients ($\chi^2_{(1)} = 7.58$; $P = 0.006$). A positive PET diagnosis distinguished AD patients from NLs with 94% sensitivity and 100% specificity (96% accuracy, $\chi^2_{(1)} = 44.2$; $P < 0.001$) and MCI patients from NLs with 68% sensitivity and 100% specificity (79% accuracy, $\chi^2_{(1)} = 23.2$; $P < 0.001$). PET accuracy was independent of dementia severity, because 14 (93%) of 15 patients with mild AD and 17 (94%) of 18 patients with moderate to

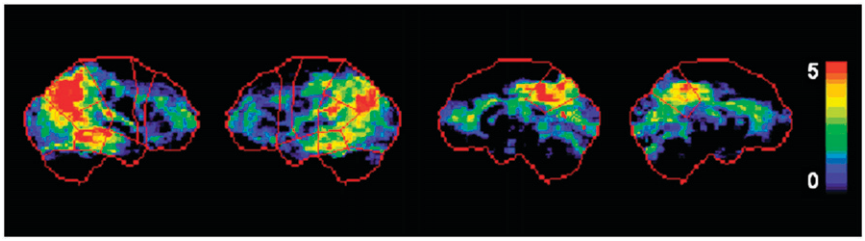

FIGURE 1. Standardized ROIs. Predefined anatomic surface ROIs (in red) are superimposed onto (from left to right) right and left lateral and right and left medial views of standardized brain template showing surface projection maps of statistical abnormalities in AD patients as compared with NLs. z scores are represented on color-coded scale ranging from 0 (black) to 5 (red). Typical AD-related CMRglc reductions in parietotemporal and posterior cingulate cortices are evident in ROIs.

TABLE 2
z Scores in Clinical Groups by Reference Database

ROI	NL		MCI		AD	
	DB^-	DB^+	DB^-	DB^+	DB^-	DB^+
IPL L	0.47 (0.23)	0.49 (0.21)	1.04 (0.93)	1.56 (0.66)*	1.48 (0.46)	2.49 (0.83)*
IPL R	0.44 (0.24)	0.48 (0.22)	0.87 (0.87)	1.25 (0.89)*	1.52 (0.91)	2.43 (0.93)*
LTL L	0.47 (0.42)	0.41 (0.23)	1.26 (0.85)	1.32 (0.91)	2.13 (0.79)	2.93 (0.35)*
LTL R	0.43 (0.38)	0.51 (0.38)	1.11 (1.08)	1.27 (0.94)*	2.16 (1.03)	2.74 (0.93)*
OCC L	0.35 (0.42)	0.32 (0.31)	0.97 (0.40)	0.05 (0.51)	1.35 (0.56)	1.40 (0.72)
OCC R	0.48 (0.61)	0.44 (0.50)	0.78 (0.65)	0.85 (0.57)	1.12 (0.66)	1.34 (0.52)
PCC L	0.71 (0.62)	0.82 (0.86)	1.10 (0.86)	1.86 (0.82)*	1.81 (0.53)	3.51 (0.45)*
PCC R	0.62 (0.76)	0.74 (0.67)	0.98 (0.89)	1.72 (0.98)*	1.50 (1.02)	2.72 (1.13)*
PFC L	0.85 (0.84)	0.73 (0.65)	1.13 (0.85)	1.10 (0.95)	1.92 (0.44)	2.28 (0.60)
PFC R	1.02 (0.75)	0.85 (0.92)	1.15 (0.79)	1.09 (0.94)	1.54 (1.08)	1.80 (1.12)
S-M L	0.40 (0.41)	0.34 (0.23)	0.44 (0.31)	0.54 (0.54)	0.47 (0.24)	0.51 (0.39)
S-M R	0.33 (0.35)	0.32 (0.33)	0.32 (0.52)	0.43 (0.57)	0.35 (0.53)	0.53 (0.50)

*DB^+ higher than DB^-, $P \leq 0.05$.

IPL = inferior parietal lobe; LTL = lateral temporal lobe; OCC = occipital cortex; PCC = posterior cingulate cortex; PFC = prefrontal cortex; S-M = sensorimotor cortex; L = left hemisphere, R = right hemisphere.

Values in parentheses are SDs.

severe AD were correctly identified ($\chi^2_{(1)} = 0.02$; $P = 0.89$, not statistically significant).

Using DB^+, all AD and MCI patients received a positive PET diagnosis, and both groups were distinguished from NLs with 100% accuracy (Fig. 3), which was significantly higher than with DB^- ($\chi^2_{\text{increment}(1)} = 11.5$; $P = 0.001$). Using DB^+ resulted in classification of more regions as hypometabolic than when DB^- was used. Specifically, the

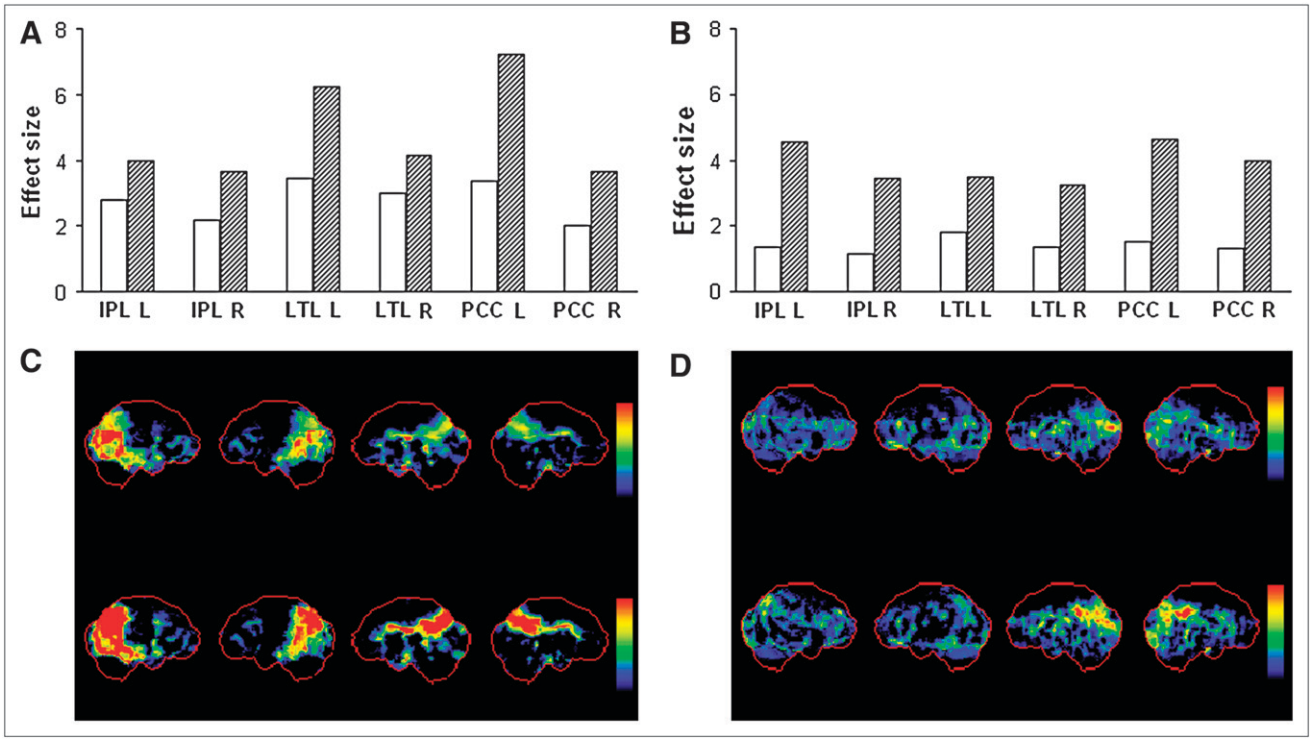

FIGURE 2. Database effects on ^{18}F-FDG PET diagnostic accuracy. (A and B) Effects in AD-affected brain regions discriminating AD patients (A) and MCI patients (B) from NLs using DB^- (white bars) and DB^+ (hatched bars). (C and D) Effects of using DB^- (top row) and DB^+ (bottom row) to create 3D-SSP maps are depicted in 2 representative AD (C) and MCI (D) patients. 3D-SSP maps showing CMRglc reductions in AD and MCI patients are displayed on same color-coded *z* score scale. IPL = inferior parietal lobe; L = left hemisphere; LTL = lateral temporal lobe; PCC = posterior cingulate cortex; R = right hemisphere.

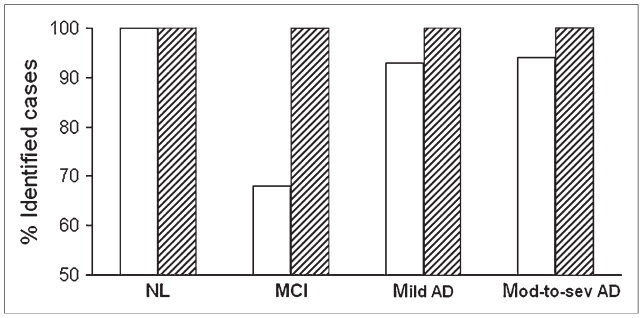

FIGURE 3. ^{18}F-FDG PET diagnostic accuracy. Percentage of NLs (n = 19), MCI patients (n = 37), patients with mild AD (n = 15), and patients with moderate to severe (mod-to-sev) AD (n = 18) correctly identified using DB$^-$ (white bars) and DB$^+$ (hatched bars).

posterior cingulate cortex appeared consistently hypometabolic in all MCI and AD subjects, and the parietotemporal CMRglc reductions were more extended and easily identifiable in patients with mild AD (Fig. 2).

DISCUSSION

The clinical utility of ^{18}F-FDG PET for the assessment of AD depends on selection of adequate reference subjects to determine with confidence whether regional CMRglc is abnormal on a single-patient basis, particularly in the early stages of disease. The present study demonstrated that the diagnostic accuracy of automated ^{18}F-FDG PET examinations in AD and MCI patients can be improved by using a reference database derived from longitudinally confirmed NLs.

Using our PET database of longitudinally stable NLs reduced the number of false-negatives without increasing the number of false-positives in diagnosing MCI and AD, as compared with a mixed database including an epidemiologically likely percentage of future MCI patients. The diagnostic sensitivity achieved with our longitudinal database was 100% for AD and MCI, whereas that of the mixed database was 94% for AD and 68% for MCI, indicating that normative values from longitudinally confirmed NLs might be particularly useful in early AD. This effect resulted from 1.4- to 2-fold increased z scores within AD-vulnerable regions, such as the posterior cingulate and parietotemporal cortices, as compared with those derived from the mixed database.

To clarify the origin of such effects, we compared the baseline ^{18}F-FDG PET scans of the 22 NL-MCI patients with 22 age-matched NL-NLs. This analysis showed CMRglc reductions in the posterior cingulate cortex and parietotemporal regions in the declining NLs, as compared with the nondeclining NLs (Fig. 4). However, these CMRglc reductions were subtle and could be detected only at an exploratory probability threshold of $0.05 \leq P < 0.01$, uncorrected for multiple comparisons (Fig. 4).

The accuracy in distinguishing MCI patients from NLs using ROI z scores was higher than the 68% accuracy of visual inspection, reaching a high of 95% for the lateral temporal lobe. This effect was likely due to the use of continuous z score variables, and thus flexible cutoff levels, as compared with routine diagnostic procedures that necessarily result in categoric variables (normal or abnormal). The present data suggest that probabilistic estimates may be a useful complement to standard diagnostic procedures.

The MCI group in our study fulfilled the criteria for amnesic MCI. Patients with amnesic MCI are a diagnostic group at elevated risk for progressing to AD (*2*) and typically present with an AD-like PET pattern, although the hypometabolism is milder than in AD (*4,18*). These MCI patients were accurately distinguished from NLs using automated ^{18}F-FDG PET examinations with the NL-NL database. It remains to be established whether this procedure would improve diagnosis of other MCI subtypes.

The mixed database was created so as to include 40% of future decliners to MCI over 4 y, according to an estimated decline rate of 10%/y (*8–12*). These estimates are derived from typical research settings, which may include enriched samples at high risk for decline. Nonetheless, databases for image analysis are typically developed in such research settings, and our study underlines the importance of carefully selecting representative NLs to create such databases.

In the present study, the PET images of NLs used in both databases were acquired on the same scanner at New York

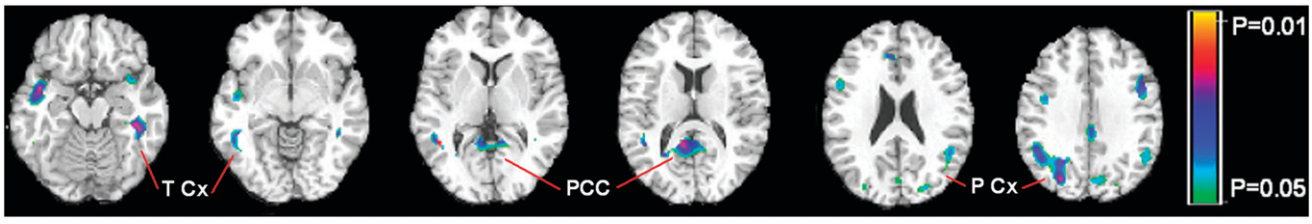

FIGURE 4. Comparison between NL-MCI patients and NL-NLs. Brain regions showing baseline CMRglc reductions in 22 NL-MCI patients and 22 age-matched NL-NLs are displayed on standardized T1-weighted MRI template in axial view (from left to right: z = 29 to z = 64 mm, every 5 mm, relative to anterior commissure–posterior commissure line). Voxelwise group comparison of spatially normalized ^{18}F-FDG PET scans was performed with t test for independent samples accounting for global CMRglc (*3,5*). CMRglc reductions in NL-MCI patients compared with NL-NLs were evident mainly in temporal, posterior cingulate, and parietal cortices. Color scale indicate P values corresponding to significance of CMRglc reductions, ranging from P = 0.05 to P = 0.01, uncorrected for multiple comparisons. PCC = posterior cingulate cortex; P Cx = parietal cortex; T Cx = temporal cortex.

University, and the scans of the testing group were acquired on a different scanner at the University of Florence. Therefore, differences in scanner resolution would have affected the detection of CMRglc abnormalities in a similar fashion in NLs, MCI patients, and AD patients from the testing group, without affecting comparison of data between databases. Previous studies have shown that multicenter ^{18}F-FDG PET discrimination of AD patients from NLs is reliable using automated procedures such as in our study (i.e., spatial normalization, image rescaling to a common voxel size, and restriction of analysis to gray-matter voxels) (*19*). Examination of data from different scanners is nonetheless necessary before we make our database available to other PET centers.

There is evidence that hippocampal CMRglc adds to the cortical regions in distinguishing NLs, MCI patients, AD patients (*17,20*), and patients with preclinical AD (*8,12*). Currently, Neurostat does not provide for direct examination of the hippocampus. Automated procedures to examine hippocampal CMRglc exist (*20*), and studies are needed to assess whether the combination of the 2 methodologies would further improve diagnostic accuracy.

CONCLUSION

Our database of longitudinally confirmed NLs constitutes a reliable ^{18}F-FDG PET normative reference for detecting MCI and early AD, by combining qualitative with quantitative estimation of CMRglc abnormalities. These results indicate a potential direct clinical value for the procedure as a diagnostic tool to facilitate clinical decision making in early AD.

ACKNOWLEDGMENTS

This study was supported by NIH-NIA AG12101, AG13616, AG08051, and AG022374; NIH NCRR MO1RR0096; and the Alzheimer's Association.

REFERENCES

1. Silverman DH, Small GW, Chang CY, et al. Positron emission tomography in evaluation of dementia: regional brain metabolism and long-term outcome. *JAMA*. 2001;286:2120–2127.
2. Petersen RC, Doody R, Kurz A, et al. Current concepts in mild cognitive impairment. *Arch Neurol.* 2001;58:1985–1992.
3. Minoshima S, Giordani B, Berent S, Frey KA, Foster NL, Kuhl DE. Metabolic reduction in the posterior cingulate cortex in very early Alzheimer's disease. *Ann Neurol.* 1997;42:85–94.
4. Drzezga A, Grimmer T, Riemenschneider M, et al. Prediction of individual outcome in MCI by means of genetic assessment and ^{18}F-FDG PET. *J Nucl Med.* 2005;46:1625–1632.
5. Minoshima S, Frey KA, Koeppe RA, Foster NL, Kuhl DE. A diagnostic approach in Alzheimer's disease using three-dimensional stereotactic surface projections of fluorine-18-FDG PET. *J Nucl Med.* 1995;36:1238–1248.
6. Signorini M, Paulesu E, Friston K, et al. Rapid assessment of regional cerebral metabolic abnormalities in single subjects with quantitative and nonquantitative [^{18}F]FDG PET: a clinical validation of statistical parametric mapping. *Neuroimage.* 1999;9:63–80.
7. Herholz K, Salmon E, Perani D, et al. Discrimination between Alzheimer dementia and controls by automated analysis of multicenter FDG PET. *Neuroimage.* 2002;17:302–316.
8. de Leon MJ, Convit A, Wolf OT, et al. Prediction of cognitive decline in normal elderly subjects with 2-[^{18}F]fluoro-2-deoxy-D-glucose/positron-emission tomography (FDG/PET). *Proc Natl Acad Sci U S A.* 2001;98:10966–10971.
9. Jagust W, Gitcho A, Sun F, Kuczynski B, Mungas D, Haan M. Brain imaging evidence of preclinical Alzheimer's disease in normal aging. *Ann Neurol.* 2006; 59:673–681.
10. Rusinek H, De Santi S, Frid D, et al. Regional brain atrophy rate predicts future cognitive decline: 6-year longitudinal MR imaging study of normal aging. *Radiology.* 2003;229:691–696.
11. Jack CR, Shiung MM, Gunter JL, et al. Comparison of different MRI brain atrophy rate measures with clinical disease progression in AD. *Neurology.* 2004; 62:591–600.
12. Mosconi L, De Santi S, Li J, et al. Hippocampal hypometabolism predicts cognitive decline from normal aging. Neurobiol Aging; 2007 Jan 10 [Epub ahead of print].
13. Mosconi L, Sorbi S, de Leon MJ, et al. Hypometabolism exceeds atrophy in presymptomatic early-onset familial Alzheimer's disease. *J Nucl Med.* 2006;47: 1778–1786.
14. Morris JC, Ernesto C, Shaefer K, et al. Clinical dementia rating (CDR) training and reliability protocol: The Alzheimer Disease Cooperative Study Unit experience. *Neurology.* 1997;48:1508–1510.
15. Reisberg B, Ferris SH, de Leon MJ, Crook T. The global deterioration scale for assessment of primary degenerative dementia. *Am J Psychiatr.* 1982;139:1136–1139.
16. Lezak MD. *Neuropsychological Assessment*. 3rd ed. New York, NY: Oxford University Press;1995.
17. Mosconi L, De Santi S, Li Y, et al. Visual rating of medial temporal lobe metabolism in mild cognitive impairment and Alzheimer's disease using FDG-PET. *Eur J Nucl Med Mol Imaging.* 2006;33:210–221.
18. Chetelat G, Desgranges B, De La Sayette V, Viader F, Eustache F, Baron JC. Mild cognitive impairment: Can FDG-PET predict who is to rapidly convert to Alzheimer's disease? *Neurology.* 2003;60:1374–1377.
19. Herholz K, Salmon E, Perani D, et al. Discrimination between Alzheimer dementia and controls by automated analysis of multicenter FDG-PET. *Neuroimage.* 2002;17:302–316.
20. Mosconi L, Tsui WH, De Santi S, et al. Reduced hippocampal metabolism in MCI and AD: automated FDG-PET image analysis. *Neurology.* 2005;64:1860–1867.